

# Phosphorus and Arsenic Impurity Centers in ZnSe. I. Paramagnetic Resonance\*

R. K. Watts, W. C. Holton, and M. de Wit  
*Texas Instruments Incorporated, Dallas, Texas 75222*  
 (Received 10 September 1970)

By means of electron paramagnetic resonance, phosphorus and arsenic impurities in ZnSe are identified to occur substitutional for selenium in crystalline material doped during growth from the melt. They are unassociated centers; however, their symmetry is lowered from  $T_d$  to  $C_{3v}$  by a Jahn-Teller distortion. Optical excitation can be used to change the density of those which are paramagnetic, i.e.,  $P_{Se}(3s^2 3p^5)$  and  $As_{Se}(4s^2 4p^5)$ .

## I. INTRODUCTION

The ability of the II-VI compounds to incorporate a wide variety of point defects is well known. These defects are of interest largely because of their effects on the electrical and optical properties of the materials. Although many magnetic defects have been studied by electron spin resonance<sup>1</sup> (ESR), there are few reports of simple acceptor centers in these crystals. Perhaps the best-known acceptor defect in the II-VI compounds is the self-activated center,<sup>1</sup> a complex formed by association of a cation vacancy and a group-III or group-VII impurity, and responsible for luminescence and for compensation of unassociated group-III or group-VII donors. The alkali metals apparently form shallow acceptors,<sup>2</sup> but they have not been observed by ESR. The exception is Li in ZnO and BeO<sup>3</sup>; in this case a distorted deep-acceptor center results, the paramagnetic hole being trapped on a nearest-neighbor oxygen. Of the group-I noble metal atoms, Cu has been shown to form a simple acceptor<sup>4,5</sup> in ZnS and CdS. Several of the other transition-metal ions also act as acceptors (for example, Cr and Yb).

This paper reports the first observation of ESR of group-V acceptors in a II-VI compound. Phosphorus and arsenic are found to form in ZnSe unassociated deep-acceptor centers whose symmetry is lowered by a Jahn-Teller distortion. The following paper discusses the observed optical and electrical effects of these group-V impurity-doped crystals, and relates some of them to the paramagnetic defects reported here.

## II. EXPERIMENTAL DETAILS

High-purity ZnSe powder was synthesized by allowing molten 6N pure zinc to react with a flowing stream of  $H_2Se$  gas. This powder was then sublimed in vacuum to a higher-density mass of more uniform stoichiometry. A small amount of arsenic or phosphorus was added, and single crystals were grown in a sealed ampoule by a gradient-freeze method.<sup>6</sup> Such a growth method is necessary because of the volatility of the dopants. The

details of this procedure are described in Ref. 6.

Single crystals were cleaved from the boules, and a {110} cleavage face was mounted parallel to the plane of rotation of the dc magnetic field. All measurements were performed with an X-band superheterodyne spectrometer, usually with the sample at 1.3 K. A light pipe of Infrasil quartz extends along the axis of the  $TE_{101}$  right circular cylindrical cavity, allowing the sample to be illuminated while the ESR signal is monitored. Illumination is provided by a 1.5-kW BH6 high-pressure mercury arc lamp and a prism monochromator. A calibrated variable diaphragm and neutral density filters in the light path allow the number of photons incident on the sample to be held constant as the wavelength is changed.

## III. SPECTRA

At 1.3 K, a characteristic ESR spectrum with axial symmetry is always observed in ZnSe crystals doped with phosphorus or arsenic. In some samples, irradiation with blue light is necessary to make the resonance appear. The largest hyperfine interaction is with a nuclear spin  $\frac{1}{2}$  in the case of phosphorus doping and  $\frac{3}{2}$  in the case of arsenic. Since phosphorus and arsenic have 100% naturally abundant isotopes with nuclear spin  $\frac{1}{2}$  and  $\frac{3}{2}$ , respectively, these resonances are assigned to phosphorus and arsenic in a  $\langle 111 \rangle$  axial field. The lines broaden and disappear as the temperature is increased. No resonance is observed above 10 K.

Figure 1 shows the phosphorus spectra with the magnetic field along a  $\langle 111 \rangle$  symmetry axis. The two lines at higher magnetic field are due to centers whose axes are parallel to the field, while the lower field doublet arises from centers whose axes are along the other  $\langle 111 \rangle$  directions making an angle of  $70.5^\circ$  with the magnetic field. The hyperfine splitting is largest along the axis and smallest perpendicular to the axis. The small satellites, which are most easily seen on the parallel spectrum, arise from interaction with six selenium nuclei. For the field along the axis, these are divided into two groups of three equivalent nuclei. The selenium superhyperfine interaction could not be analyzed in

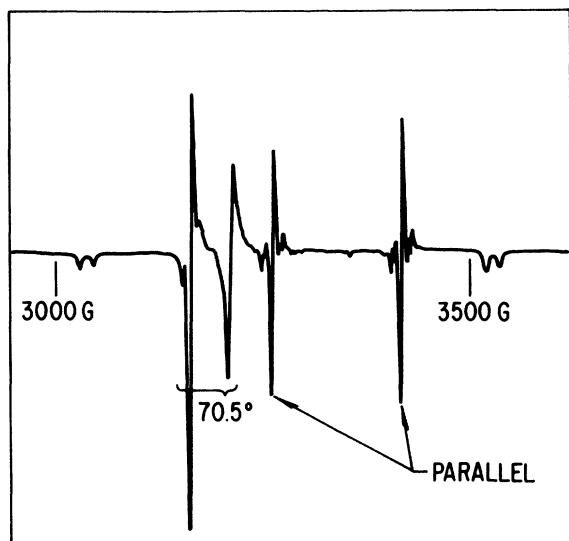


FIG. 1. Phosphorus spectra at 9 GHz and 1.3 K with magnetic field parallel to a  $\langle 111 \rangle$  direction. The lines due to centers with symmetry axes along the field are marked parallel; those from centers whose symmetry axes are the other three  $\langle 111 \rangle$  directions are marked  $70.5^\circ$ .

detail because only for the field near  $\langle 111 \rangle$  are the lines well resolved. In addition, there is an axial superhyperfine interaction with one zinc nucleus along the axis.

The spin Hamiltonian describing the spectrum of a center is written

$$\mathcal{H} = \beta \vec{H} \cdot \vec{g} \cdot \vec{S} + \vec{I} \cdot \vec{A} \cdot \vec{S} + \vec{I}^{\text{Zn}} \cdot \vec{K}^{\text{Zn}} \cdot \vec{S} + \sum_{i=1}^6 \vec{I}_i^{\text{Se}} \cdot \vec{K}_i^{\text{Se}} \cdot \vec{S},$$

$$S = \frac{1}{2} \quad (1)$$

where  $A$ ,  $K^{\text{Zn}}$ , and  $K^{\text{Se}}$  represent the hyperfine interactions with P, Zn, and Se nuclei, respectively. The values of the constants are given in Table I.

The small, saturated lines near the 3000- and 3500-G field marks in Fig. 1 are not part of the spectrum of interest; they are more easily studied at 77 K where saturation of the lines is not a problem. They are due to a center displaying a large ( $\sim 600$  G) nearly isotropic hyperfine interaction with a spin- $\frac{1}{2}$  nucleus and a much smaller hyperfine interaction with three other spin- $\frac{1}{2}$  nuclei, which are equivalent when the magnetic field is along a  $\langle 111 \rangle$  axis. Details of this center will be published elsewhere. It will be labeled tentatively "P<sub>4</sub>" for the purposes of this discussion, since it may be

TABLE I. Resonance parameters for ZnSe:P.

$g_{\parallel} = 1.9989 \pm 0.0003$	$g_{\perp} = 2.1074 \pm 0.0003$
$A_{\parallel} = (146 \pm 1) \times 10^{-4} \text{ cm}^{-1}$	$A_{\perp} = (8.3 \pm 0.5) \times 10^{-4} \text{ cm}^{-1}$
$K_{\parallel}^{\text{Zn}} = (11.0 \pm 0.1) \times 10^{-4} \text{ cm}^{-1}$	$K_{\perp}^{\text{Zn}} = (4.6 \pm 1.1) \times 10^{-4} \text{ cm}^{-1}$
$K^{\text{Se}} = 15.23 \times 10^{-4} \text{ cm}^{-1}$ for $\vec{H} \parallel \langle 111 \rangle$	

due to a cluster of four phosphorus ions with the paramagnetism localized mainly on one phosphorus. In a sample from which the P<sub>4</sub> spectrum is absent, the sensitivity of the phosphorus spectrum to optical irradiation was studied. The resonance is enhanced most by 0.50- $\mu$  light and quenched most by 0.9–1.04- $\mu$  light. Figure 2 shows these effects. The resonance is seen before illumination at 1.3 K in this sample.

When uniaxial stress is applied along  $\langle 111 \rangle$ , the parallel spectra increase in intensity and the  $70.5^\circ$  lines decrease correspondingly. Since this redistribution of population occurs at 1.3 K where ions are immobile, defect association can be ruled out as the origin of the trigonal distortion.

Figure 3 shows the spectra of the similar arsenic center. The  $70.5^\circ$  pattern is complicated because of a large quadrupole interaction. The spectrum is described by the Hamiltonian of Eq. (1) with the addition of a quadrupole term

$$Q(I_x^2 - \frac{1}{3}I^2 - \frac{1}{3}I^2).$$

The values of the parameters are given in Table II. The values of the quadrupole parameter  $Q$  and  $A_{\perp}$  were found by comparing the angular dependence of the spectrum with that calculated for different choices of  $A_{\perp}$  and  $Q$ . Observation of the  $\Delta m_I = \pm 1$  transitions made this method practical, because the angular dependence of these transitions is quite sensitive to the values of  $A_{\perp}$  and  $Q$ .

When small amounts of iron are present in the samples, the spectrum of an iron-arsenic associate is observed. Fe<sup>3+</sup> substitutes for zinc and As<sup>3-</sup> replaces a nearest-neighbor selenium, producing a  $\langle 111 \rangle$  axial center. The paramagnetism is concentrated almost entirely on the iron. No analogous iron-phosphorus center is seen. This spectrum

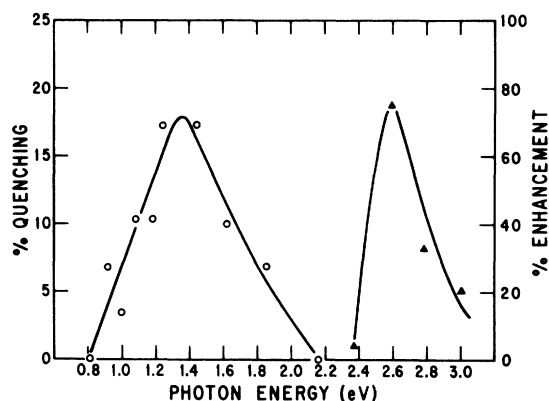


FIG. 2. Enhancement (triangles) and quenching (dots) of phosphorus ESR signal upon illumination of the sample with light of various energies, the photon flux into the sample remaining constant. The curves merely indicate the trend of the data.

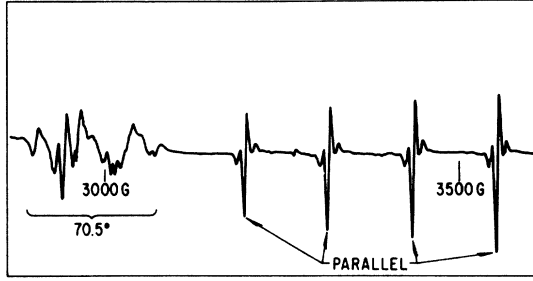


FIG. 3. Arsenic spectra at 9 GHz and 1.3 K. The magnetic field is parallel to a  $\langle 111 \rangle$  direction, and spectra from the different centers are marked as in Fig. 1.

has been reported in detail elsewhere.<sup>7</sup>

#### IV. DISCUSSION

The ground states of the  $p^n$  configurations ( $n=1-5$ ) in a trigonal field were examined theoretically. Matrices of spin-orbit, trigonal-field, and inter-electronic-electrostatic interaction energies were diagonalized, and wave functions and  $g$  factors calculated as described in the Appendix for the ground states for ranges of the parameters characterizing these energies. Only for the  $p^5$  configuration do  $g$  factors matching the observations occur. It seems most likely that phosphorus or arsenic would occur substitutional for selenium. The electronic configuration would be  $ns^2np^5$ , and the ion would behave as a simple neutral acceptor.

On this model, the seleniums with which interactions are seen are the six next nearest neighbors which do not lie in the nodal plane of the  $p$  orbital of the hole. An alternative model has phosphorus interstitial at the interstice with four nearest-neighbor zincs and six next-nearest-neighbor seleniums. But this model is less appealing since it requires a doubly charged interstitial. If the outer  $s$  electrons of neutral phosphorus were promoted to the  $p$  shell to give a  $p^5$  configuration, then the interstitial would have no charge. Such a promotion occurs for iron-group interstitials in silicon<sup>8</sup> with a change of principal quantum, however. In the cases of arsenic and phosphorus, the energy necessary for promotion is from two to twenty times greater,<sup>9</sup> however, and therefore we discard this model.

The wave function of the paramagnetic hole can

TABLE II. Resonance parameters for ZnSe:As.

$g_{  } = 1.9363 \pm 0.0010$	$g_{\perp} = 2.2173 \pm 0.0017$
$A_{  } = (108.2 \pm 1.0) \times 10^{-4} \text{ cm}^{-1}$	$A_{\perp} = (28 \pm 5) \times 10^{-4} \text{ cm}^{-1}$
$Q = (21 \pm 4) \times 10^{-4} \text{ cm}^{-1}$	$K_{\perp}^{2B} = (3.8 \pm 2.0) \times 10^{-4} \text{ cm}^{-1}$
$K_{  }^{2A} = (14.1 \pm 0.4) \times 10^{-4} \text{ cm}^{-1}$	
$K^{6s} = 15.21 \times 10^{-4} \text{ cm}^{-1}$ for $\vec{H} \parallel \langle 111 \rangle$	

be written

$$\psi = \sum_i \alpha_i \Phi_i, \quad (2)$$

where

$$\Phi_i = \beta_i s_i + (1 - \beta_i^2)^{1/2} p_i \quad (3)$$

and  $i$  labels the various atoms with which interaction is observed.  $s_i$  and  $p_i$  are  $s$  and  $p$  orbitals of atom  $i$ . The components of the hyperfine tensors are

$$K_{||}^i = a_i \alpha_i^2 \beta_i^2 + 2b_i \alpha_i^2 (1 - \beta_i^2), \quad (4)$$

$$K_{\perp}^i = a_i \alpha_i^2 \beta_i^2 - b_i \alpha_i^2 (1 - \beta_i^2),$$

where

$$a_i = 8\pi |s_i(0)|^2 \mu_i / 3I_i, \quad (5)$$

$$b_i = 2\langle r^{-3} \rangle_p \mu_i / 5I_i \text{ in G,}$$

and  $\mu_i$  and  $I_i$  are the nuclear moment and spin of atom  $i$ . If core polarization is ignored and the  $s$  orbital density at the nucleus and  $\langle r^{-3} \rangle$  for the  $p$  orbitals are known, then the occupation of the  $s$  and  $p$  orbitals,  $\alpha^2 \beta^2$  and  $\alpha^2 (1 - \beta^2)$ , respectively, can be calculated from the measured hyperfine parameters.

The Hartree-Fock values of Clementi<sup>10</sup> for the  $3s$  and  $3p$  orbitals of  $P^-$  and the  $4s$  and  $4p$  orbitals of  $As^-$  were scaled according to the procedure of Knight<sup>11</sup> in order to find values of  $a$  and  $b$  for  $P^{2-}$  and  $As^{2-}$ . For the  $4s$  and  $4p$  orbitals of  $Zn^{2+}$ , the Hartree-Fock values of Froese<sup>12</sup> for  $Zn^0$  were scaled. Since Knight's table<sup>11</sup> contains no scaling factor for zinc, the factor given for gallium was used.

Since the signs of the measured hyperfine parameters are not known, values of  $\alpha^2$  and  $\beta^2$  were computed for both possible choices of relative signs. Because of overlap among the functions  $\Phi_i$ , the quantity  $\sum_i \alpha_i^2$  need not equal unity. Although the selenium interaction could not be analyzed in detail, there may be appreciable hole density on the six seleniums. The values of the densities for equal signs add to 1.1 for phosphorus and 0.75 for arsenic according to Table III. In view of the approximations made, these values seem reasonable. The hole is largely concentrated in a  $p$  orbital of

TABLE III. Densities in  $s(\alpha^2 \beta^2)$  and  $p[\alpha^2 (1 - \beta^2)]$  orbitals inferred from hyperfine data (see text). The relative signs of  $A$  and  $B$  are not known.

Atom	$A/B > 0$		$A/B < 0$	
	$\alpha^2 \beta^2$	$\alpha^2 (1 - \beta^2)$	$\alpha^2 \beta^2$	$\alpha^2 (1 - \beta^2)$
P	0.017	0.90	0.014	1.0
Zn	0.009	0.17	0.001	0.38
As	0.019	0.55	0.007	0.87
Zn	0.008	0.17	0.002	0.34

arsenic or phosphorus.

Some insight into the nature of the axial distortion can perhaps be gained from consideration of a severely distorted configuration of the tetrahedral cluster of phosphorus (or arsenic) and its four nearest-neighbor zincs in which the phosphorus and three of the zincs are coplanar. (Phosphorus is assumed to substitute for selenium.) In this case the  $s$  and two of the  $p$  orbitals of phosphorus make  $sp^2$  bonds with the zincs in the plane, and there is a half-filled phosphorus  $p$  orbital whose axis is perpendicular to the plane. As the distortion is relaxed to the perfect tetrahedral  $sp^3$  case, more  $s$  character is acquired by the half-filled orbital. From the data of Table III, the angle between the axial bond and a basal bond is found to be  $96^\circ$  for phosphorus. It is  $90^\circ$  for  $sp^2$  and  $110^\circ$  for  $sp^3$  bonding. Thus, the distortion may be such that the phosphorus and three of the neighboring zincs are nearly coplanar.

A simple model of the origin of the distortion will now be given. The normal vibrational coordinates of a tetrahedral cluster span the  $a_1$ ,  $e$ , and  $2t_2$  (called  $t_2^a$  and  $t_2^b$ ) representations of  $T_d$ . The symmetrized product of  $\sigma$  orbitals spans  $2a_1$ ,  $e$ , and  $2t_2$ ; therefore, a  $\sigma$  orbital can interact with all the normal coordinates of the cluster. Interaction with an  $e$  mode leads to  $\langle 100 \rangle$  distortions, and interaction with a  $t_2$  mode to  $\langle 111 \rangle$  distortions. The displacements are along the bonds only for  $a_1$  and  $t_2^a$  distortions, and, hence, these should couple most strongly to  $\sigma$  orbitals. The components of  $t_2^a$  are, in Sturge's<sup>13</sup> notation,

$$\begin{aligned} Q_4 &= \frac{1}{2}(z_1 - z_2 + z_3 - z_4), \\ Q_5 &= \frac{1}{2}(z_1 + z_2 - z_3 - z_4), \\ Q_6 &= \frac{1}{2}(z_1 - z_2 - z_3 + z_4). \end{aligned} \quad (6)$$

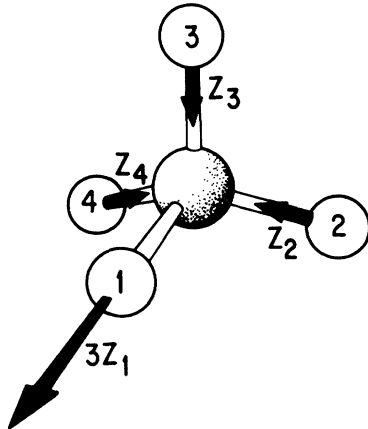


FIG. 4. Illustration of distortion of Eq. (11) (see text). The central ball represents phosphorus or arsenic and the others, zincs.

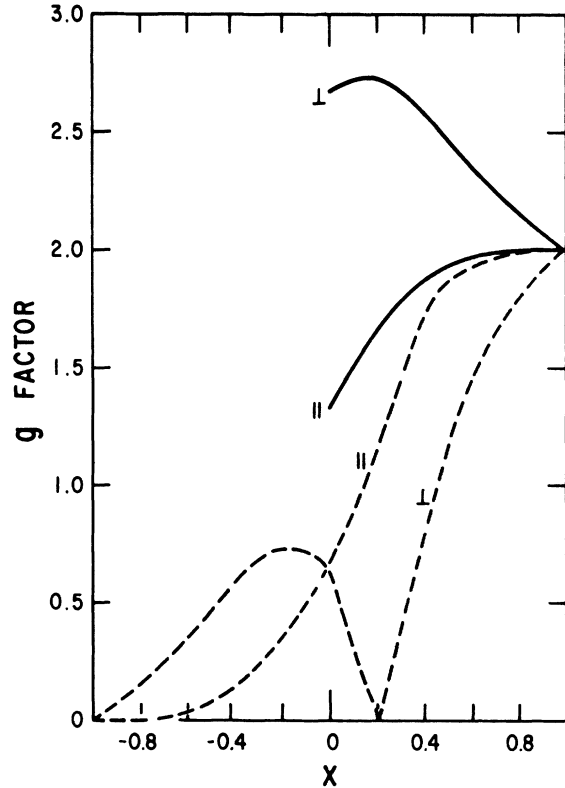


FIG. 5. Calculated  $g_{II}$  and  $g_I$  for the ground doublet of the  $p^1$  configuration (dashed) and of the  $p^5$  configuration (solid) in a trigonal electric field. The  $g$  factors are plotted vs  $X$ , where  $X = \nu(1 + |\nu|)^{-1}$  and  $\nu = B/\zeta$  (see text). For  $X < 0$  the ground doublet of  $p^5$  has  $g_I = 0$ ; it is, thus, of no interest and its  $g$  factors are not plotted.

$z_i$  is the displacement of neighbor  $i$  along the bond direction, an outward displacement away from the phosphorus being positive. The component of the  $a_1$  mode is

$$Q_1 = \frac{1}{2}(z_1 + z_2 + z_3 + z_4). \quad (7)$$

If the electronic system is assumed to interact strongly only with these two modes, the Hamiltonian representing this interaction can be written

$$\begin{aligned} \mathcal{H}' &= E_0 + Q_1 \left( \frac{\partial E}{\partial Q_1} \right)_0 + \sum_{i=4}^6 Q_i \left( \frac{\partial E}{\partial Q_i} \right)_0 \\ &\quad + \frac{1}{2} \kappa_t \sum_{i=4}^6 Q_i^2 + \frac{1}{2} \kappa_1 Q_1^2. \end{aligned} \quad (8)$$

$E_0$  represents the static energy which is a function of mean nuclear positions and the nuclear kinetic energy;  $E$  depends upon the displacements of the nuclei of the cluster. The last two terms are the elastic potential energy of the two modes. In order that  $\mathcal{H}'$  transform as  $a_1$ , Eq. (8) must have the form

$$\begin{aligned} \mathcal{H}' &= E_0 + c_1 Q_1 + c_t (Q_4 yz + Q_5 zx + Q_6 xy) \\ &\quad + \frac{1}{2} \kappa_1 Q_1^2 + \frac{1}{2} \kappa_t \sum_{i=4}^6 Q_i^2, \end{aligned} \quad (9)$$

where  $x, y, z$  are electronic coordinates and  $c_i$  and  $c'_i$  are electronic-vibrational coupling constants. The matrix of Eq. (9), based on the  $s$  and  $p$  orbitals of which  $\sigma$  bonds are composed, is

$$\begin{array}{cccc} s & p_x & p_y & p_z \\ V & 0 & 0 & 0 \\ 0 & V & c'_1 Q_6 & c'_1 Q_5 \\ 0 & c'_1 Q_6 & V & c'_1 Q_4 \\ 0 & c'_1 Q_5 & c'_1 Q_4 & V \end{array} \quad (10)$$

$c'_i$  is proportional to  $c_i$  and

$$V = c_1 Q_1 + \frac{1}{2} \kappa_1 Q_1^2 + \frac{1}{2} \kappa_t \sum_{i=4}^6 Q_i^2 + E_0.$$

The breathing mode  $Q_1$  only shifts the energy zero. Minimization of the lowest root of the secular equation with respect to the orientation of  $Q_4, Q_5, Q_6$  leads to an eigenvalue  $Q_m$  of the distortion

$$\begin{aligned} Q_m &= (Q_4 + Q_5 + Q_6)/\sqrt{3} \\ &= (3z_1 - z_2 - z_3 - z_4)/\sqrt{3}. \end{aligned} \quad (11)$$

This distortion is shown in Fig. 4. If the central atom is allowed to move to keep the center of mass stationary, the central atom and atoms 2-4 tend toward a coplanar arrangement.

#### V. SUMMARY

Phosphorus and arsenic have been shown to form isolated deep-acceptor centers in ZnSe. At low temperature the hole is observed to be trapped on the acceptor, and a distortion of the surroundings is evident. Although a complete theory of such a covalent complex interacting with vibrational modes

is not developed, a simple model appears adequate to explain the essential features observed.

These centers are rather similar to the self-activated centers in halogen-doped  $\text{ZnS}_{1-x}\text{Se}_x$  mixed crystals<sup>1</sup> in which the unpaired spin is localized on a single selenium. The  $g$  factors are similar, the orbital of the spin has almost entirely  $p$  character, and the selenium is bound to its three zinc neighbors by  $sp^2$  bonds also.

#### ACKNOWLEDGMENT

We thank R. D. Stinedurf for growing the sample crystals.

#### APPENDIX

In this Appendix the energy levels and ground-state  $g$  factors for the  $p^n$  electronic configurations are examined when a trigonal electrostatic field is present in order to see which configurations have doublets with  $g$  factors near those found for ZnSe:P and ZnSe:As. The trigonal field  $A \sum_i (3z_i^2 - r_i^2)$ , where the sum is over the electrons  $i$  of the configuration, transforms into the operator-equivalent Hamiltonian

$$\mathcal{H}_T = B \sum_i (3l_{zi}^2 - 2), \quad (A1)$$

where  $B = -2A \langle r^2 \rangle_p / 5$ . The Hamiltonian of interest is obtained by adding the spin-orbit interaction to (A1):

$$\mathcal{H} = \mathcal{H}_T + \sum_i \xi \hat{L}_i \cdot \hat{S}_i. \quad (A2)$$

The  $p^1$  configuration contains one multiplet,  $^2P$ . The matrix of  $\mathcal{H}$  among the six states  $|M_L M_S\rangle$  is

$$\begin{array}{cccccc} 1\frac{1}{2} & 1 - \frac{1}{2} & 0\frac{1}{2} & 0 - \frac{1}{2} & -1\frac{1}{2} & -1 - \frac{1}{2} \\ \left[ \begin{array}{cccccc} B + \frac{1}{2}\xi & & & & & \\ & B - \frac{1}{2}\xi & \xi/\sqrt{2} & & & \\ & \xi/\sqrt{2} & -2B & & & \\ & & & -2B & \xi/\sqrt{2} & \\ & & & \xi/\sqrt{2} & B - \frac{1}{2}\xi & \\ & & & & & B + \frac{1}{2}\xi \end{array} \right] \end{array} \quad (A3)$$

The energies of the three doublets were calculated as a function of the parameter  $B/\xi$ . The same state is lowest over the entire range  $B/\xi = -\infty$  to  $B/\xi = \infty$ . The  $g$  factors of this doublet are shown in Fig. 5 (dashed curves). For no value of  $B/\xi$  do  $g$  factors similar to the experimental one occur.

Matrix (A3) serves also for the  $p^5$  configuration if  $\xi$  is replaced by  $-\xi$ . In this case the two lowest-energy levels cross at  $B/\xi = 0$ . For  $B/\xi < 0$  the ground doublet has  $g_1 = 0$ . For  $B/\xi > 0$  the  $g$  factors are as shown in Fig. 5 (solid curves).  $g$  factors near the experimental ones are found for  $B/\xi \approx 1-2$  (As) and  $B/\xi \approx 5$  (P).

The  $p^2$  and  $p^4$  configurations have multiplets  $^3P$ ,  $^1S$ , and  $^1D$ , the  $^3P$  being lowest. The matrix of  $\mathcal{H}$  among the  $^3P$  states is, for  $p^2$ ,

$$\begin{array}{cccccccc}
 11 & 10 & 1-1 & 01 & 00 & 0-1 & -11 & -10 & -1-1 \\
 \left[ \begin{array}{cccccccc}
 -B + \frac{1}{2}\zeta & & & & & & & & \\
 & -B & & \frac{1}{2}\zeta & & & & & \\
 & & -B - \frac{1}{2}\zeta & & \frac{1}{2}\zeta & & & & \\
 & \frac{1}{2}\zeta & & 2B & & & & & \\
 & & \frac{1}{2}\zeta & & 2B & & \frac{1}{2}\zeta & & \\
 & & & & 2B & & & \frac{1}{2}\zeta & \\
 & & & \frac{1}{2}\zeta & & -B - \frac{1}{2}\zeta & & & \\
 & & & & \frac{1}{2}\zeta & & & -B & \\
 & & & & & & & & -B + \frac{1}{2}\zeta
 \end{array} \right]
 \end{array} \quad (A4)$$

All doublets have  $g_1 = 0$ .

The  $p^3$  configuration has multiplets  $^4S$ ,  $^2D$ , and  $^2P$  with  $^4S$  lowest.  $^4S$  is not split by  $\mathcal{H}$  in first order, but  $\mathcal{H}$  can mix the other multiplets into  $^4S$ . The matrix of  $\mathcal{H} + \sum_{i,j} e^2 r_{ij}^{-1}$  among the three multiplets decomposes into submatrices, one being, for example,

$$\begin{array}{ccccc}
 S0 \frac{1}{2} & P1 - \frac{1}{2} & P0 \frac{1}{2} & D1 - \frac{1}{2} & D0 \frac{1}{2} \\
 \left[ \begin{array}{ccccc}
 -9F & -\zeta/\sqrt{3} & -2\zeta/\sqrt{6} & & \\
 -\zeta/\sqrt{3} & 6F & & 3B + \frac{1}{2}\zeta & -\zeta/\sqrt{6} \\
 -2\zeta/\sqrt{6} & & 6F & \zeta/\sqrt{2} & -\zeta/\sqrt{3} \\
 & 3B + \frac{1}{2}\zeta & \zeta/\sqrt{2} & & \\
 & -\zeta/\sqrt{6} & -\zeta/\sqrt{3} & & 
 \end{array} \right],
 \end{array} \quad (A5)$$

where  $F = F^2/25$ . The  $\pm \frac{3}{2}$  doublet has  $g_1 = 0$  and the  $\pm \frac{1}{2}$  doublet has, for reasonable values of  $B$ ,  $\zeta$ , and  $F$ ,  $g_{\parallel} = 2$ ,  $g_{\perp} = 4$ . Thus,  $p^5$  is the only configuration with ground-state  $g$  factors near the experimental values.

\*Research sponsored in part by the Air Force Office of Scientific Research Contract No. F-44620-67-C-0073.

<sup>1</sup>ESR studies of II-VI compounds are reviewed in R. S. Title, in *Physics and Chemistry of II-IV Compounds*, edited by M. Aven and J. S. Prener (North-Holland, Amsterdam, 1967); J. Schneider, in *II-VI Semiconducting Compounds*, edited by D. G. Thomas (Benjamin, New York, 1967).

<sup>2</sup>J. Dieleman, J. W. DeJong, and T. Meyer, *J. Chem. Phys.* **45**, 3178 (1966).

<sup>3</sup>O. F. Schirmer, *J. Chem. Phys. Solids* **29**, 1407 (1968).

<sup>4</sup>I. Broser and H. Maier, *J. Phys. Soc. Japan Suppl.* **21**, 254 (1966).

<sup>5</sup>M. de Wit, *Phys. Rev.* **177**, 441 (1969).

<sup>6</sup>W. C. Holton, R. K. Watts, and R. D. Stinedurf,

*J. Crys. Growth* **6**, 97 (1969).

<sup>7</sup>R. K. Watts, *Phys. Rev. B* **2**, 1239 (1970).

<sup>8</sup>G. W. Ludwig and H. H. Woodbury, in *Solid State Physics*, edited by F. Seitz and D. Turnbull (Academic, New York, 1962), Vol. 13, Chap. 4.

<sup>9</sup>C. E. Moore, *Atomic Energy Levels* (U. S. GPO, Washington, D. C., 1949).

<sup>10</sup>E. Clementi, *IBM J. Res. Develop.* **9**, 2 (1965).

<sup>11</sup>W. D. Knight, in *Solid State Physics*, edited by F. Seitz and D. Turnbull (Academic, New York, 1957), Vol. 2, Chap. 2.

<sup>12</sup>C. Froese, *J. Chem. Phys.* **45**, 1417 (1966).

<sup>13</sup>M. D. Struge, in *Solid State Physics*, edited by F. Seitz and D. Turnbull (Academic, New York, 1967), Vol. 20, Chap. 3.